TRANSFORM DOMAIN PROCESSING FOR DIGITAL COMMUNICATION SYSTEMS USING SURFACE ACOUSTIC WAVE DEVICES.

(12)

(9) Technical Report MA-ARO-3 (14)

by

(10) L. B. Milstein, D. R. Arsenault and P. Das

(11) 15 May 1978 (12) 18 p.

U. S. Army Research Office
Grant DAAG-29-77-G-0205 (15)

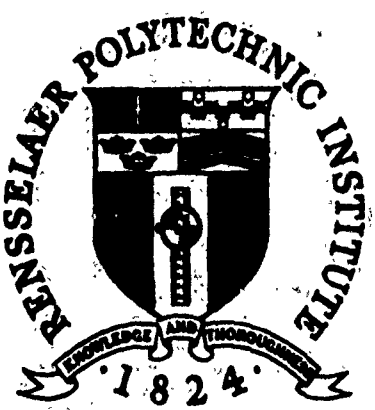

Electrical and Systems Engineering Department
Rensselaer Polytechnic Institute
Troy, New York 12181

SECURITY CLASSIFICATION OF THIS PAGE (When Data Entered)

REPORT DOCUMENTATION PAGE

READ INSTRUCTIONS BEFORE COMPLETING FORM

1. REPORT NUMBER: ~~MA-ARO-3~~	2. GOVT ACCESSION NO.
3. RECIPIENT'S CATALOG NUMBER	
4. TITLE (and Subtitle): TRANSFORM DOMAIN PROCESSING FOR DIGITAL COMMUNICATIONS SYSTEMS USING SURFACE ACCOUSTIC WAVE DEVICES	5. TYPE OF REPORT & PERIOD COVERED: Technical Report
	6. PERFORMING ORG. REPORT NUMBER
7. AUTHOR(s): L.B. Milstein, D.R. Arsenault and P. Das	8. CONTRACT OR GRANT NUMBER(s): DAAG -29-77-G-0205
9. PERFORMING ORGANIZATION NAME AND ADDRESS: Electrical and Systems Engineering Department, Rensselaer Polytechnic Institute, Troy, NY 12181	10. PROGRAM ELEMENT, PROJECT, TASK AREA & WORK UNIT NUMBERS
11. CONTROLLING OFFICE NAME AND ADDRESS: U. S. Army Research Office, Post Office Box 12211, Research Triangle Park, NC 27719	12. REPORT DATE: May 15, 1978
	13. NUMBER OF PAGES: Fifteen (15)
14. MONITORING AGENCY NAME & ADDRESS(if different from Controlling Office)	15. SECURITY CLASS. (of this report): UNCLASSIFIED
	15a. DECLASSIFICATION/DOWNGRADING SCHEDULE

16. DISTRIBUTION STATEMENT (of this Report)

Approved for public release; distribution unlimited.

17. DISTRIBUTION STATEMENT (of the abstract entered in Block 20, if different from Report)

18. SUPPLEMENTARY NOTES

The findings in this report are not to be construed as an official Department of the Army position, unless so designated by other authorized documents.

19. KEY WORDS (Continue on reverse side if necessary and identify by block number)

spread spectrum communication system, adaptive, SAW technology

78 12 04 009

20. ABSTRACT (Continue on reverse side if necessary and identify by block number)

The use of surface acoustic wave (SAW) devices in communication systems has recently been receiving a reasonable amount of attention. This is because SAW devices can be used to perform accurate real-time convolutions of broadband waveforms, thus enabling them to function efficiently as matched filters, Fourier transformers, etc. In particular, they appear to have a tremendous potential in spread spectrum systems.

In the past, these devices have been shown to be capable of narrowband (Cont.)

DD FORM 1 JAN 73 1473 EDITION OF 1 NOV 65 IS OBSOLETE

interference removal by Fourier transforming the received signal, passing the resulting waveform through either a notch-filter or a hard limiter, and then inverse transforming the latter signal.

In this paper, a variety of extensions of previous results will be demonstrated. One of the key limitations of processing signals in the Fourier transform domain with SAW devices is the fact that only finite segments in time of the input waveform can be transformed by the device. It will be shown that by separating the data into two parallel bit streams, this problem can be avoided.

To illustrate the interference rejection properties of the device when used as a real-time Fourier transformer, experimental results will be presented illustrating the narrowband interference rejection referred to above. Probability of error curves for a system employing a 7 bit Barker encoded binary PSK waveform embedded in additive Gaussian noise and operating both with and without the presence of a narrowband jammer will be presented. However, because of equipment limitations these latter measurements were not made with contiguous data.

The relevance of this type of technology to avionics is relatively clear. These devices are light enough and small enough to be used on board aircraft, and the ability to receive contiguous-time digital signals accurately and securely is certainly of prime importance in avionics.

TRANSFORM DOMAIN PROCESSING FOR DIGITAL COMMUNICATION SYSTEMS USING SURFACE ACOUSTIC WAVE DEVICES*

L. B. Milstein
Department of Applied Physics and Information Science
University of California, San Diego
La Jolla, California

D. R. Arsenault and P. Das
Electrical and Systems Engineering Department
Rensselaer Polytechnic Institute
Troy, New York

SUMMARY

The use of surface acoustic wave (SAW) devices in communication systems has recently been receiving a reasonable amount of attention. This is because SAW devices can be used to perform accurate real-time convolutions of broadband waveforms, thus enabling them to function efficiently as matched filters, Fourier transformers, etc. In particular, they appear to have a tremendous potential in spread spectrum systems.

In the past, these devices have been shown to be capable of narrowband interference removal by Fourier transforming the received signal, passing the resulting waveform through either a notch-filter or a hard limiter, and then inverse transforming the latter signal.

In this paper, a variety of extensions of previous results will be demonstrated. One of the key limitations of processing signals in the Fourier transform domain with SAW devices is the fact that only finite segments in time of the input waveform can be transformed by the device. It will be shown that by separating the data into two parallel bit streams, this problem can be avoided.

To illustrate the interference rejection properties of the device when used as a real-time Fourier transformer, experimental results will be presented illustrating the narrowband interference rejection referred to above. Probability of error curves for a system employing a 7 bit Barker encoded binary PSK waveform embedded in additive Gaussian noise and operating both with and without the presence of a narrowband jammer will be presented. However, because of equipment limitations these latter measurements were not made with contiguous data.

The relevance of this type of technology to avionics is relatively clear. These devices are light enough and small enough to be used on board aircraft, and the ability to receive contiguous-time digital signals accurately and securely is certainly of prime importance in avionics.

1. INTRODUCTION

This paper is concerned with the detection of digital signals in the presence of additive Gaussian noise and interference. Classically, analog filtering techniques are performed by convolving the signal to be filtered by the impulse response of the filter. Recently, a new approach to analog filtering (Milstein, L.B., 1977) has been suggested, one that relies on the ability of some device, in this case, a surface acoustic wave (SAW) device, to perform a real-time Fourier transformation (and/or Fourier inversion), thereby enabling one to filter in the "frequency domain" by multiplication of appropriate Fourier transforms rather than in the "time domain" by convolution. This filtering in the frequency domain allows one the flexibility of employing filters which could not be implemented in the time domain (i.e., are unrealizable). In particular, receivers using ideal bandpass filtering and ideal notch filtering have been investigated (Das, P., 1977).

In this paper there will be a review of SAW devices in the next section, followed by a survey of some of the techniques of implementing transformations with SAW devices. The actual receiver under consideration will be presented in Section 4 and, in Section 5, experimental results will be presented showing how the receiver is capable of suppressing narrowband interference (modeled as a sine wave). Finally, Section 6 will summarize the results that have been achieved to date and indicate the directions that this technology appears to be taking in the future.

2. REVIEW OF SURFACE ACOUSTIC WAVE TECHNOLOGY

Surface acoustic waves have been well known and well studied by the seismologists since Lord Rayleigh's discovery of this mode of wave propagation in 1895. Only in the last two decades (Ultrasonics Symposium Proceedings, 1972-1976), however, has the importance of SAW in the electronic industry been realized. This is due to two main factors. First is the availability of piezoelectric substrates like lithium niobate ($LiNbO_3$), and lead zirconium titanate (PZT), and second is the easy generation and reception of SAW on a piezoelectric substrate using interdigital transducers. Thus, one can easily make a delay line with an insertion loss of a few dBs, tens of microseconds of delay, and a center frequency which varies from 10 MHz to a few gigahertz. It is to be mentioned that one can also make a delay line using bulk ultrasound (i.e., using a device wherein the wave travels through the entire volume rather than just near the surface), but there are two very important reasons why a SAW delay line is more attractive. First of all, the SAW can be very easily tapped on a piezoelectric substrate by one interdigital transducer (or a set of transducers) to make a tapped delay line. In addition, one can put independent tapping weights on the pick-off points. This makes the realization of transversal or finite impulse response (FIR) filters with pre-specified characteristics (within certain limitations) very simple. Thus, using the well-known techniques of digital filter design, one can design a single mask which, employing the usual process of photolithography (well developed by the integrated circuits industry), can be used to manufacture these filters with significant reduction in cost.

SAW technology includes not only Rayleigh waves, but all the waves which can propagate on a solid surface somewhat confined near the surface. For Rayleigh waves the confinement is of the order of one wavelength (for $LiNbO_3$ at 100 MHz, $\lambda \sim 30\ \mu$), but for other waves, like Blustein-Gulayev waves, the confinement length may be much larger, say $\epsilon_r \lambda$, where ϵ_r is the effective relative dielectric constant which, for example, is approximately 30 for $LiNbO_3$. Rayleigh waves on a perfect surface of piezoelectric insulator are non-dispersive and non-dissipative, but in actual solids the dispersion and loss characteristics become of importance in the gigahertz region. For frequencies less than 500 MHz, of much more importance is the alignment of the crystallographic axes with the direction of wave propagation. This is because in an anisotropic solid, the directions of the energy and the wave vectors are collinear only in certain specified directions and for large misalignment of the vectors, significant amounts of energy travel at an angle away from the desired direction. Also, for high frequencies, diffraction loss may become significant.

An oscillator can be made using a SAW delay line and an external amplifier. The Q of this delay line oscillator is generally of the order of a few thousand. For higher Q oscillators, one uses so-called SAW resonators. The resonators are made of one or two interdigital transducers with many metal fingers or grooves to be used as reflective arrays for the planar cavity. With proper care, oscillator Qs of the order of 60,000 have been reported (Bell, D.T., 1976).

The basic advantage for the SAW devices discussed above is that they use planar technology and thus can be cheaply mass-produced. For the tapped delay line applications, one major handicap is the rather large temperature coefficient of $LiNbO_3$ or other high coupling material which has low insertion loss. If one is willing to sacrifice the efficiency, ST-cut quartz is available which has zero first order temperature coefficient. Finally, there is another class of SAW devices which use acousto-electric interaction of SAW and free carriers on a semiconductor surface in a sandwich structure of semiconductor on piezoelectric substrate (i.e., silicon on $LiNbO_3$). This is discussed below.

SAW propagating on a piezoelectric substrate (i.e., delay line) interacts with carriers in a neighboring semiconductor. This interaction takes place even though the piezoelectric and semiconducting media have their surface mechanically isolated by an air gap. The acousto-electric or space charge coupling is achieved through the electric field which accompanies the surface wave. This wave exists outside the piezoelectric substrate and can penetrate inside the semiconductor and thus induce space-charge.

Accustic surface wave convolvers are real-time analog ultrasound signal processors using this interaction. A silicon-on-lithium niobate ($LiNbO_3$) structure (a so-called separate media structure) is the implementation most used. Devices of this type include (in addition to convolvers) correlators, match filters, Fourier transformers, ambiguity function generators, and phase comparators (Bers, A., 1974)(Ingebrigtsen, K., 1975)(Defranould, Ph., 1976)(Das, P., 1977)(Das, P., 1972)(Wang, W., 1972)(Otto, O., 1972)(Kino, G., 1976).

To illustrate the operation of this device, consider the situation in Fig. 1, where an RF signal $f(t)e^{j\omega t}$ is applied to one input transducer to generate a traveling wave. At the other end of the device, the input applied is $g(t)e^{j\omega t}$. These two waves, while traveling under the semiconductor, induce a propagating electric field and a space charge which can be represented at any point x and t inside the medium (to within a multiplicative factor) by

$$f(t - \tfrac{x}{v})e^{j(\omega t - kx)} \text{ and } g(t + \tfrac{x}{v})e^{j(\omega t + kx)}$$

where k is the propagation constant of the wave and v is its velocity. In overlapping, these waves interact and the current density inside the semiconductor consists of the fundamental and higher order harmonics. The output is proportional to the integral of the current density with respect to x. Thus, if only the second harmonic term is detected, the output is proportional to

$$\int_{-L/2}^{L/2} f(t - \tfrac{x}{v})\, g(t + \tfrac{x}{v})\, dx = v \int_{t-L/2V}^{t+L/2V} f(\tau)\, g(2t - \tau)\, d\tau \qquad (1)$$

where L is the physical length of the device. For time-limited signals, with $T = L/2V$, the above expression represents convolution, except for an output time compression factor of two; thus Fig. 1 depicts a convolver.

An important feature of these real-time analog signal processors is that they are programmable in the sense that one convolver can be used for many types of signals. This certainly is a great advantage over the tapped delay line correlators discussed earlier, as the latter are capable of responding to a fixed signal form only.

Finally, one other class of space-charge-coupled devices has been developed recently, the so-called memory or storage devices (Bers, A., 1974)(Ingebrigtsen, K., 1975)(Defranould, Ph., 1976)(Das, P., 1977), which can perform the signal processing functions mentioned earlier with a stored signal in the charge pattern of a vidicon diode array placed on a $LiNbO_3$ delay line. The storage device is shown in Fig 2. To store the signal f(t), it is applied at input 1 as an envelope modulating a carrier at frequency ω. Another short input pulse (sometimes referred to as a "write-in" pulse) at frequency ω is applied either at input 2 (case 1) or at the output terminal (case 2) such that the waves generated by the signal and the write-in pulse interact to produce a DC current. This DC current produces a trapped periodic charge density due to the charging of capacitors associated with the diode arrays. The period of this charge is $(1/2k)$ for case 1 and $(1/k)$ for case 2.

The charge pattern may remain stored from seconds to ten minutes depending on the type of diode structure and the ambient temperature. To read out the stored signal, a read-in short pulse at frequency 2ω (case 1) is applied at either terminal 3 or 4. Alternately a short pulse at frequency ω (case 2) can be applied to either terminal 1 or 2. The stored signal is recovered at the output terminal. To convolve a signal g(t) with the stored signal, the short read-in pulse is replaced by g(t) and applied at either input 4 or input 2. Alternately, to correlate, g(t) is applied at either 3 or 1.

In summary, research in this area has brought real-time signal processors from the drawing board to the actual application stage. Figure 3 shows a complete unit which has been fabricated and tested with the following specifications: 100 MHz convolver; 10 μsec interaction time; 25 MHz bandwidth; insertion loss 40 dB.

3. FOURIER TRANSFORMATION USING SAW DEVICES

Fourier transformation is accomplished in real-time by a SAW device in the following manner: If a signal $f(t)e^{j(\omega t+\Delta t^2)}$ (that is, a waveform f(t) modulating a linear FM or chirp waveform) is convolved with the signal $e^{j(\omega t-\Delta t^2)}$, the result of that convolution will be the Fourier transform of f(t)(Milstein, L., 1977) (Das, P., 1977). Therefore, if these two waveforms are used as the two inputs to the SAW convolver described in the previous section, the convolver output, assuming f(t) is time-limited to some value $T \leq A$, where A is the interaction time of the device (and equals the physical length of the device divided by the velocity of propagation of the SAW in the device), will be F(ω), the Fourier transform of f(t), over the range $\omega\in[\Omega\Delta T, \Omega\Delta]$(Milstein, L., 1977). Alternately, rather than use the convolver, if one implements a tapped delay line with tap coefficients given by samples of the unmodulated chirp signal spaced (π/ω_0) seconds apart, where ω_0 is the bandwidth of the chirp waveform, one can obtain F(ω) as the output of the delay line when $f(t)e^{j(\omega t+\Delta t^2)}$ is the input. In either case, the radian frequency variable ω will be a linear function of time, so that F(ω) will be generated at the device output in real-time.

The above technique is sufficient only if the waveform is time limited to a small enough value. When the waveform is a sequence of contiguous pulses as is typical of most digital communication systems, some means of altering the procedure is clearly necessary, and one such scheme is described below.

Basically, the technique consists of dividing the input alternately into two data streams, processing each data stream separately, and then combining the results at the end. Conceptually, it is a straightforward technique, but from an implementation point of view there were a variety of subtleties involving such things as the accurate generation of constant envelope chirps in the two parallel branches and minimization of crosstalk effects in inverse transforming that had to be addressed.

Figure 4(a) shows a detailed block diagram of the system and Fig. 4(b) shows the signals at different points in the system. A chirp clock plus a delayed version of that clock controls the system as follows: The delayed clock is used to trigger a flip-flop which in turn triggers two out-of-phase impulse generators. These impulses modulate an RF carrier and then generate two out-of-phase chirp streams after passing through the two chirp filters. A second flip-flop is triggered by the non-delayed clock and is used to gate the two chirp streams so that overlapping does not occur. The streams are changed to the opposite slope by mixing with f_M. The signal s(t) is then made to modulate these streams. The modulated chirps are fed into two chirp filters from which emerges two out-of-phase Fourier transform streams. Mixing again with f_M to obtain the opposite slope, summing the two streams together, and feeding this signal into another chirp filter gives the original continuous signal at the output. The out-of-phase chirp streams are then summed together and mixed with the recovered signal to eliminate the chirp carrier. Synchronization is obtained by slightly changing the chirp stream frequency, which is independent of the signal frequency. The signal can be monitored by triggering on the signal clock, whereas the chirps are monitored by triggering on the chirp clock.

Finally, as described in (Milstein, L., 1977), (Arsenault, D., 1977), two further points are worth emphasizing. The first is obvious, merely being that since one obtains a transform valid only over a finite range in frequency, one can only inverse transform over that range in frequency so that in general, one obtains at the output of an inverse transform the desired inverse convolved with a sin x/x type weighting function.

The second point is that since in either the forward transform or inverse transform case, the transformation only appears at the output of the device when the input waveform is fully contained in the device, if the nominal carrier frequency of both the upward and downward chirps are the same, the values f(0)(and immediate vicinity) and F(0)(and immediate vicinity) cannot be obtained. Therefore, appropriate time and frequency shifting procedures have to be employed (Milstein, L., 1977) and (Arsenault, D., 1977). Alternately, if F(0) is desired, it can be obtained by using different carrier frequencies for the opposite going chirps. However, this then puts the entire range of frequencies for which an accurate transform is obtained in the vicinity of baseband rather than at RF.

4. RECEIVER STRUCTURE

The general form of the receiver is shown in Fig. 5(a). It consists of a Fourier transformer, a multiplier, an inverse Fourier transformer, and a matched filter. In essence, the filtering by the transform function H(ω) is done by multiplication followed by inverse transformation rather than by convolution. This multiplication, while ostensibly being performed in the "frequency domain", is of course, accomplished by the SAW device in real-time.

Alternately, the receiver may be implemented as shown in Fig. 5(b) (Das, P., 1977)(Otto, G., 1976), wherein the matched filtering is performed by inverse transforming the product of the transforms of the filtered input waveform and the impulse response of the matched filter.

To illustrate the above ideas, Fig. 6 shows results of narrowband interference removal when s(t) is a 13-bit Barker code sequence. (Actually, the code was composed of ONEs and ZEROs rather than ± ONES.) The interference in this case was a sine wave, and it was filtered out by multiplication in frequency by a rectangular pulse (i.e., a low-pass filter).

It can be seen from the figure that the interference has been effectively eliminated. The distortion seen in the final trace is due in large part to the bandwidth of the final video filter. As an incidental

result, if traces 1 and 3 are compared with each other (also traces 4 and 6) one can see the fidelity with which the Fourier transforms can be taken.

Figure 7 shows the actual implementation used to generate the above results, ar corresponds to the block diagram of Fig. 5(a). The Fourier transforms were implemented using SAW delay lines with a chirp impulse response built into the tap weights. However, the final matched filtering operation was performed using a silicon-on-lithium niobate convolver.

To demonstrate the feasibility of Fig. 5(b), the receiver shown in Fig. 8 was built and results are shown in Figs. 9 and 10. Figure 9 shows the output of a filter matched to a 255-bit PN code (again implemented with ONEs and ZEROs) when the input was that same code under interference-free conditions. When a narrow-band interferer (specifically a periodic triangular waveform) was added, the filter output is shown in Fig. 10.

5. EXPERIMENTAL RESULTS

The receiver structure shown in Fig. 5(b) can be implemented using less components as shown in Fig. 11 (Otto, O. W., 1976). The difference between this implementation and that of Fig. 8 is that no time-reversed signal is required for correlation. Also it is to be noted that the output of the receiver is dechirped. This is shown in Fig. 12 where both the correlation and dechirped correlation of 7-bit Barker code signals are shown. The performance of this receiver in the presence of high level jamming is also shown in Fig. 13.

To test the performance of this receiver, the probability of error curve was measured using the block diagram shown in Fig. 14. The signal used in the error-analysis was a $(2^{24} - 1)$ bit PN code generated by a 24-bit shift register. Each +1 bit of the signal was encoded with a 7-bit Barker code having dechirped correlation peak shown in Fig. 12, whereas for the 0-bit, a 180° phase shifter was used to obtain a negative correlation spike. This was done by inverting the output of the 7-bit Barker code generator with every +1 bit of the PN code generator and leaving it unchanged with a zero bit. The other output of the 7-bit code generator was used in the reference channel. The correlation output was applied to the threshold detecting and error-counting circuit shown in Fig. 15. The threshold level was set to zero and the output of the zero level detector was compared with the input signal. If there was an error it was counted in an 8-segment decade counter. The clock frequency for the signal was 2 KHz and the 7-bit Barker code was 23 μsec long (unfortunately, equipment limitations prevented these measurements from being performed with contiguous time data). The center frequency and bandwidth of the chirp filters were 15 MHz and 6 MHz respectively. The jamming noise was generated by using a sinusoidal oscillator. The RMS noise voltage was measured by a Dumont type 405 high frequency RMS voltmeter. This voltmeter was found to have high frequency resonances and to eliminate this, a 6 MHz low pass filter was inserted at the output of the noise generator. Since the system bandwidth was also 6 MHz, this still could be looked upon as more or less white noise.

Figure 16 shows the probability of error curves obtained for the system. Curve B was obtained using 0.145 volt RMS noise and 0.2 V peak to peak signal. Curves C and D show the degradation of the receiver in the presence of different jammer levels. Curves E and F show the improvement obtained by selective gating in the Fourier domain. Curve A shows the probability of error for an optimum receiver.

Comparing curves A and B, one finds that the present receiver is inferior to the optimum one by 3.5 dB. The antijamming capability is 0.5 dB and 2.5 dB for the low and high level jammers respectively. These results are preliminary and better performance can be expected by optimizing the system. For example, it is expected that curves E and F should be much closer to each other than shown in the figure. The reason this was not so in the present system was due to an improper gating of the jamming signal in the receiver. This resulted in spreading of the jammer in the frequency domain and thus could not be removed completely without degrading the signal itself.

6. DISCUSSION

Different implementations of a spread spectrum receiver using SAW devices as Fourier transformers have been discussed. For a particular implementation a probability of error curve was obtained. These are only preliminary results and no attempt has been made to compare them with theoretical predictions. The results presented in this paper are characteristic of the behavior of SAW devices as signal processors showing their superiority in situations that other devices, at present, might find troublesome to contend with. The fact that these devices allow access to the real-time Fourier transform of the signal as an automatic consequence of the correlation process (as has been demonstrated in this paper) allows one to employ such powerful techniques as filtering by transform gating and noise optimization or 'prewhitening' by multiplying the transform by a function related to the noise characteristics.

One very important advantage in the use of SAW devices for signal processing is the possibility of fabricating entire receivers, and the like, on a single substrate. For instance, all the chirp filters depicted in the correlation system of Fig. 11 can be fabricated as a single monolithic unit. From this one can envision dramatic decreases in the bulk of such systems. At the moment it seems plausible to state that the dynamic range of such systems, as have been discussed in this paper, is ultimately limited by other system components such as mixers since SAW devices are known to possess wide dynamic ranges. Although SAW devices may require high level inputs this does not present too much of a problem due to the present availability of excellent wideband high-gain amplifiers.

Finally, it should be mentioned that although the Fourier transform has been stressed solely in this paper, other transforms are also implementable using SAW devices (Arsenault, D., 1977), opening up new avenues for application.

*Partially supported by U. S. Army Research Office Grant No. DAAG-29-77-G-0205.

REFERENCES

ARSENAULT, D.R., P. Das, 1977, "SAW Fresnel Transform Devices and Their Applications", Ultrasonics Symposium Proceedings, p. 969.

BELL, D.T., and R. C. Li, 1976, "Surface Acoustic Wave Resonators", Proc. IEEE, Vol. 64, p. 711.

BERS, A., and J. H. Cafarella, 1974, "Surface Wave Correlator-Convolver with Memory", Ultrasonics Symposium Proceedings, p. 778.

DAS, P. and D. R. Arsenault, 1977, "SAW Space-Charge-Coupled-Signal-Processing and Transform Device with Storage", Extended Abstract, Electrochemical Society, Vol. 77-1, p. 112.

DAS, P., D. R. Arsenault and L. B. Milstein, 1977, "Adaptive Spread Spectrum Receiver using SAW Technology", DAAG-29-77-G-0205, Technical Report MA-ARO-1.

DAS, P., M. H. Araghi and W. C. Wang, 1972, "Convolution of Signals using Surface Wave Delay Lines", Appl. Phys. Letters, Vol. 21, p. 152.

DEFRANOULD, Ph., H. Gautier, C. Maerfeld and P. Tournois, 1976, "P-N Noise Memory Correlator", Ultrasonics Symposium, p. 336.

INGEBRIGTSEN, K. A. and E. Stern, 1975, "Holographic Storage of Acoustic Surface Waves with Schottky Diode Arrays", Ultrasonics Symposium Proceedings, p. 212.

KINO, G.S., 1976, "Acoustoelectric Interactions in Acoustic Surface Wave Devices", Proc. IEEE, Vol. 64, p. 724.

MILSTEIN, L.B. and P. Das, 1977, "Spread Spectrum Receiver using Surface Acoustic Wave Technology", IEEE Trans. Communications, Vol. COM-25, p. 841.

OTTO, O.W., 1976, "The Chirp Transform Signal Processor", Ultrasonics Symposium Proceedings, p. 365.

OTTO, O.W., 1972, "Real Time Fourier Transform with a Surface Wave Convolver", Electron Letters, Vol. 8, p. 623.

1972 Ultrasonics Symposium Proceedings.

1973 Ultrasonics Symposium Proceedings.

1974 Ultrasonics Symposium Proceedings.

1975 Ultrasonics Symposium Proceedings.

1976 Ultrasonics Symposium Proceedings.

WANG, W.C. and P. Das, 1972, "Surface Wave Convolver Via Space Charge Nonlinearity", Proceedings of the IEEE Ultrasonics Symposium, p. 316.

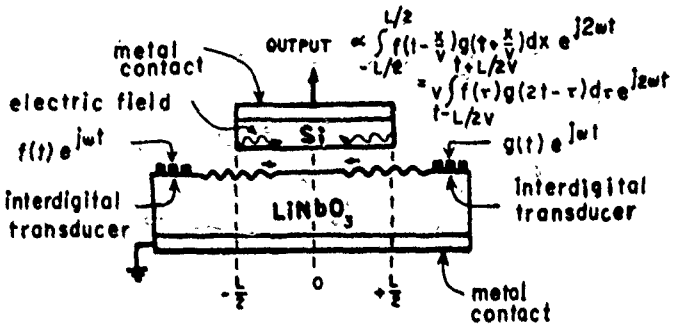

Fig. 1 The Si-on-$LiNbO_3$ Convolver Structure

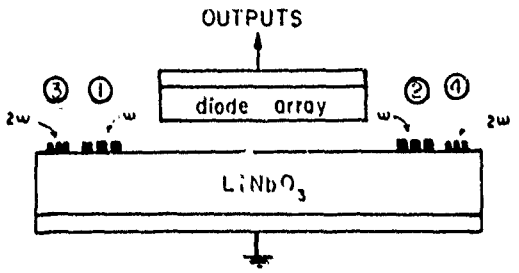

Fig. 2 The Structure of the Si-on-$LiNbO_3$ Memory Correlator

Fig. 3 External Appearance of a Si-on-$LiNbO_3$ Convolver with 100 MHz Center Frequency, 25 MHz Bandwidth and 10 μs Interaction Time

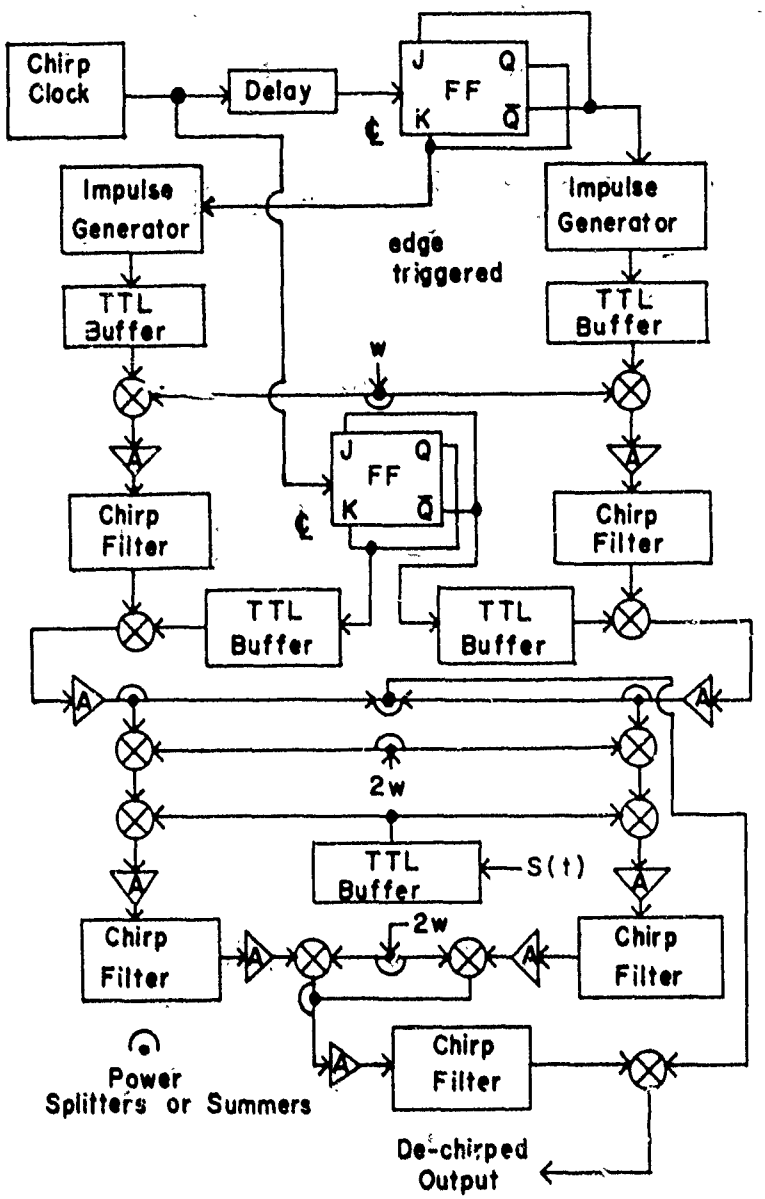

Fig. 4(a) Detailed Block Diagram of the Fourier Transformation Scheme for Continuous Signals. Gating the transform to remove unwanted frequency components is performed prior to the last chirp filter.

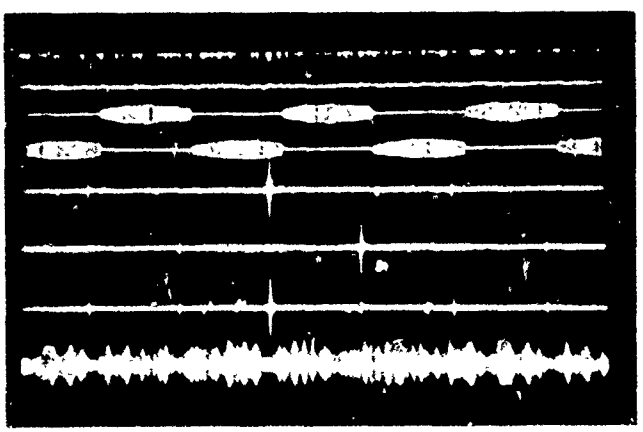

Transformation System. Type 1 is a

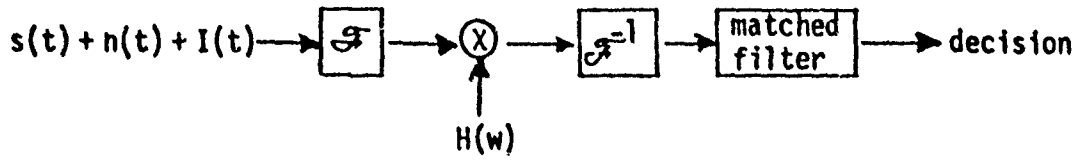

(a)

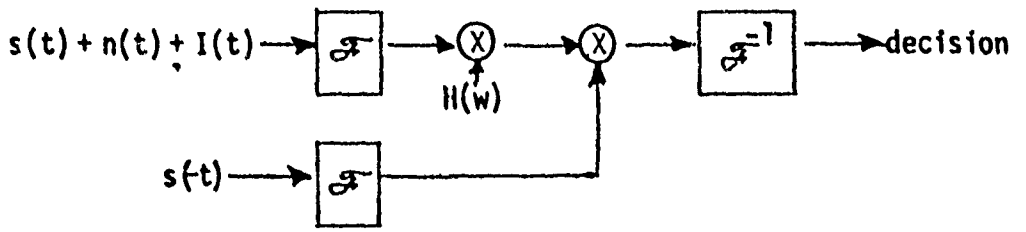

Fig. 5 Receiver Block Diagrams

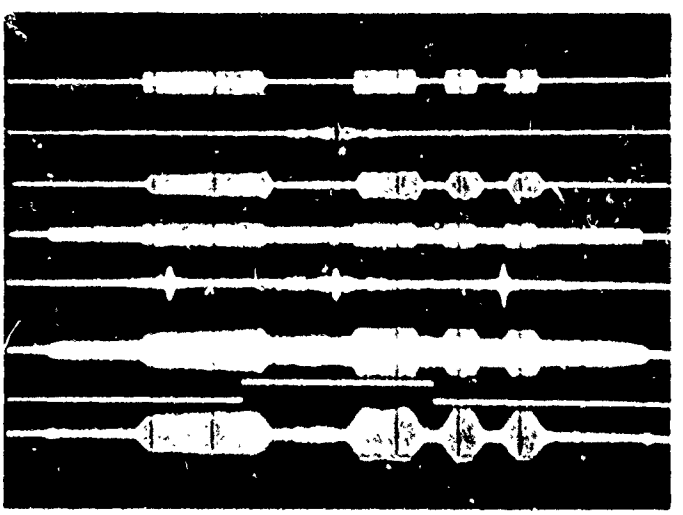

Fig. 6 Filtering of Barker Code Signal (hor. scale - 5 μsec/div.). Trace 1 - Barker Code Input; Trace 2 - Fourier Transform of Trace 1; Trace 3 - Inverse Fourier Transform of Trace 2; Trace 4 - Barker Code Plus Interference; Trace 5 - Fourier Transform of Trace 4; Trace 6 - Inverse Transform of Trace 5; Trace 7 - H(ω) - Gating Signal; Trace 8 - Filtered Signal.

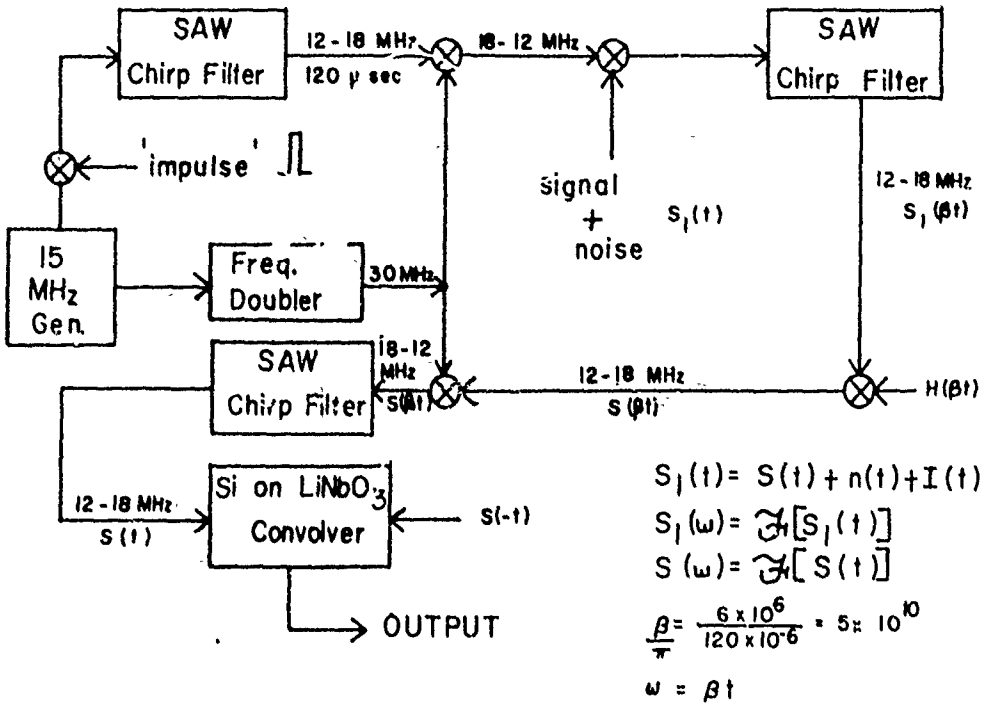

Fig. 7 Implementation of a SAW Receiver where the Matched Filter is a Si-on-$LiNbO_3$ Convolver.

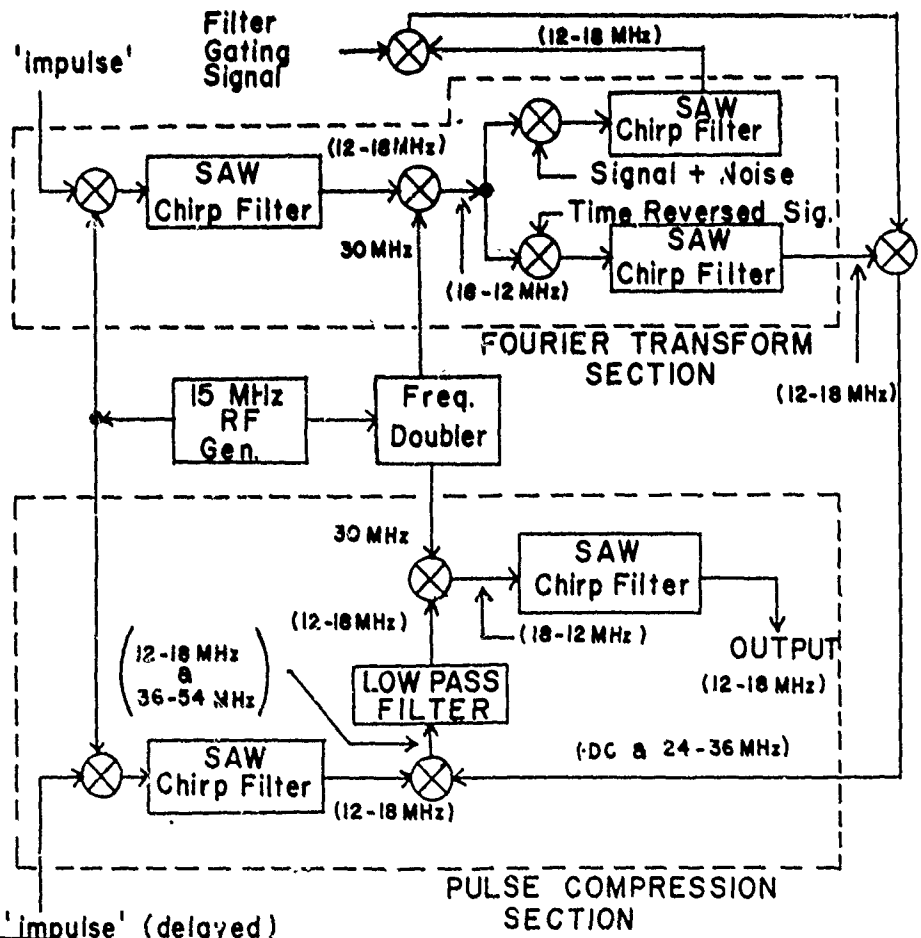

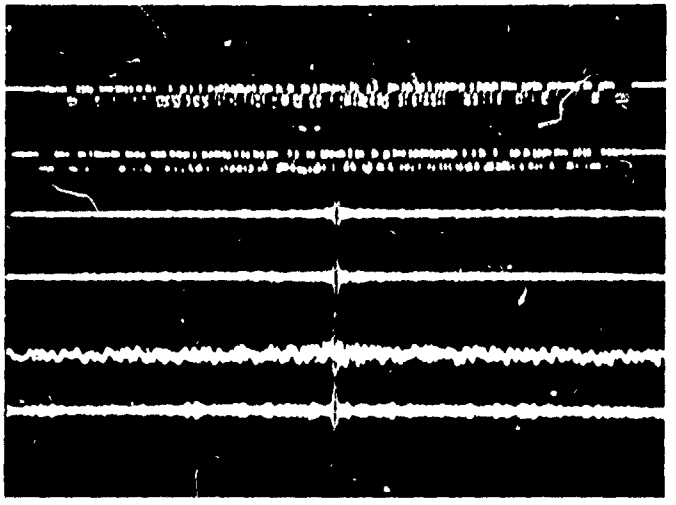

(a)

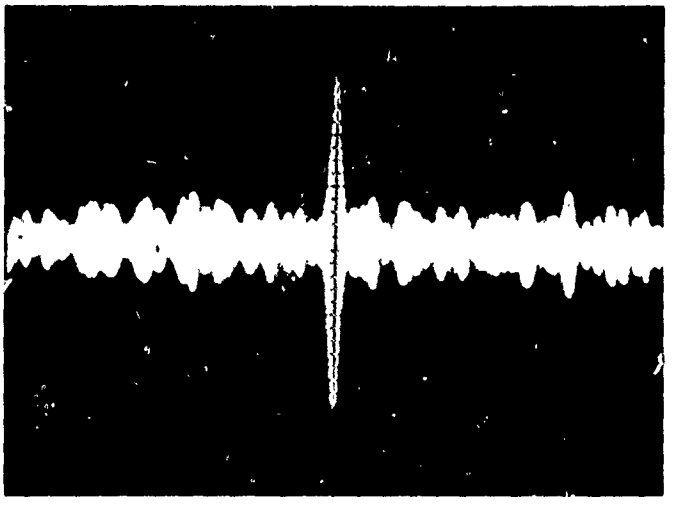

(b)

Fig. 9 255-Bit PN Code-Matched Filtering. (a) Hor. scale - 5 μsec/div., Traces 1 and 2 - Code and Its Time Reversal; Traces 3 and 4 - Respective Fourier Transforms; Trace 5 - Product of Traces 3 and 4; Trace 6 - Matched-Filtered Output. (b) Magnified and Expanded View of Trace 6 (hor. scale - 2 μsec/div.

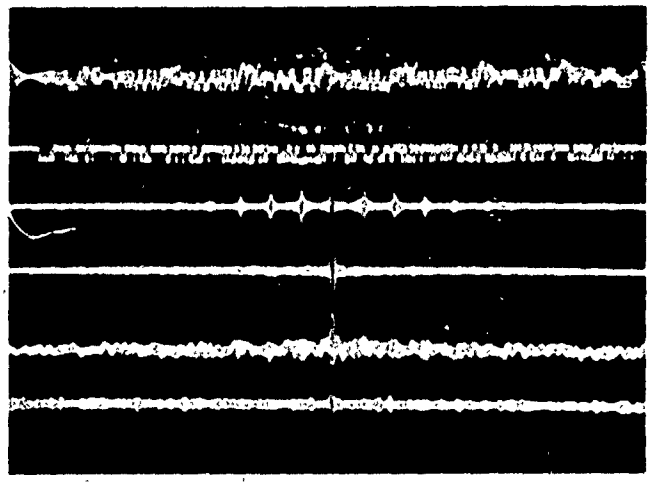

Fig. 10 255-Bit PN Code-Matched Filtering in the Presence of Triangular Interferer (hor. scale - 5 μsec/div.). Trace 1 - Signal Plus Interferer; Trace 2 - Time Reversed Signal; Traces 3 and 4 Fourier Transforms of 1 and 2 Respectively; Trace 5 - Multiplication of Traces 3 and 4; Trace 6 - Matched-Filtered Output.

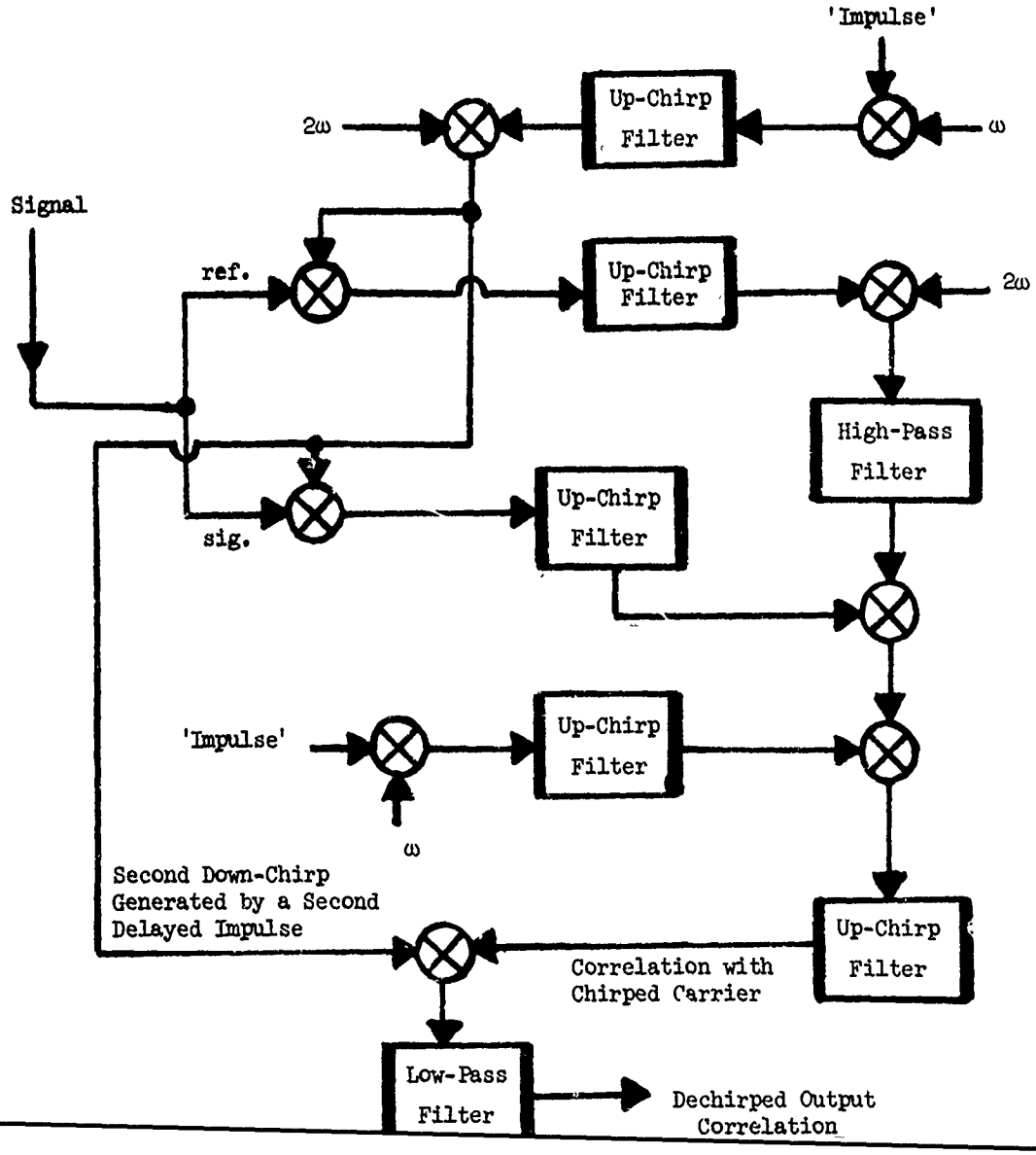

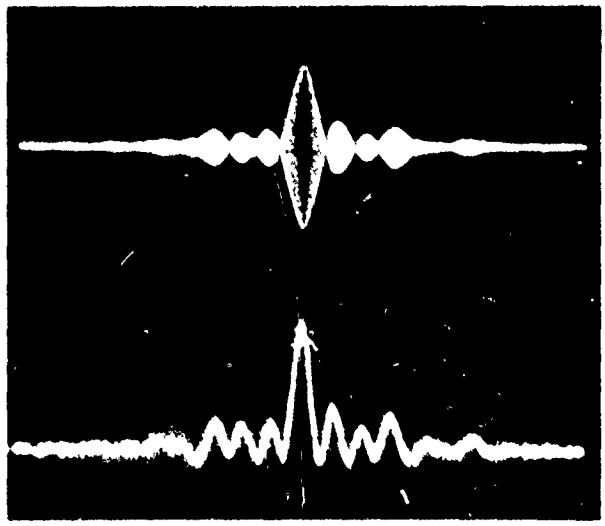

Fig. 12 Output Correlation of the 7-Bit Barker Code from the System with and without the Chirped Carrier which is Removed by Coherent Detection.

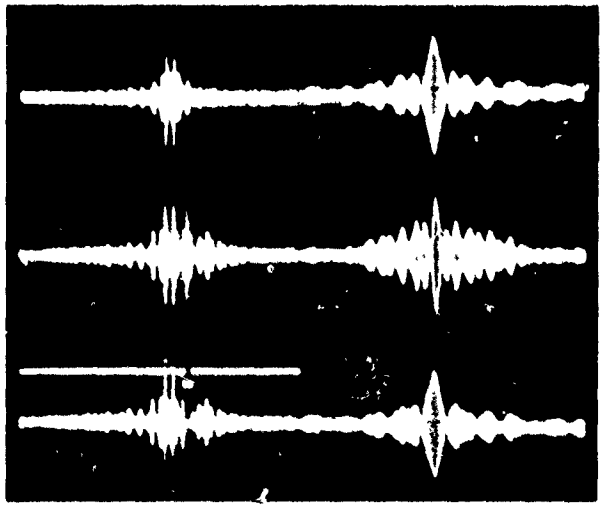

Fig. 13 The Removal of a High-Level Jammer by Notching of the Fourier Transform in a Matched Filter. Trace 1 left - The Positive Side of a 7-bit Barker Code Fourier Transform; Trace 1 right - Output Correlation; Trace 2 left - Fourier Transform with Large Component due to a Monochromatic Jammer; Trace 2 right - Distorted Output Correlation due to Jammer; Trace 3 - Notch for the Elimination of the Jammer from the Fourier Transform, Trace 4 left - Notched Fourier Transform; Trace 3 right - Filtered Output Correlation.

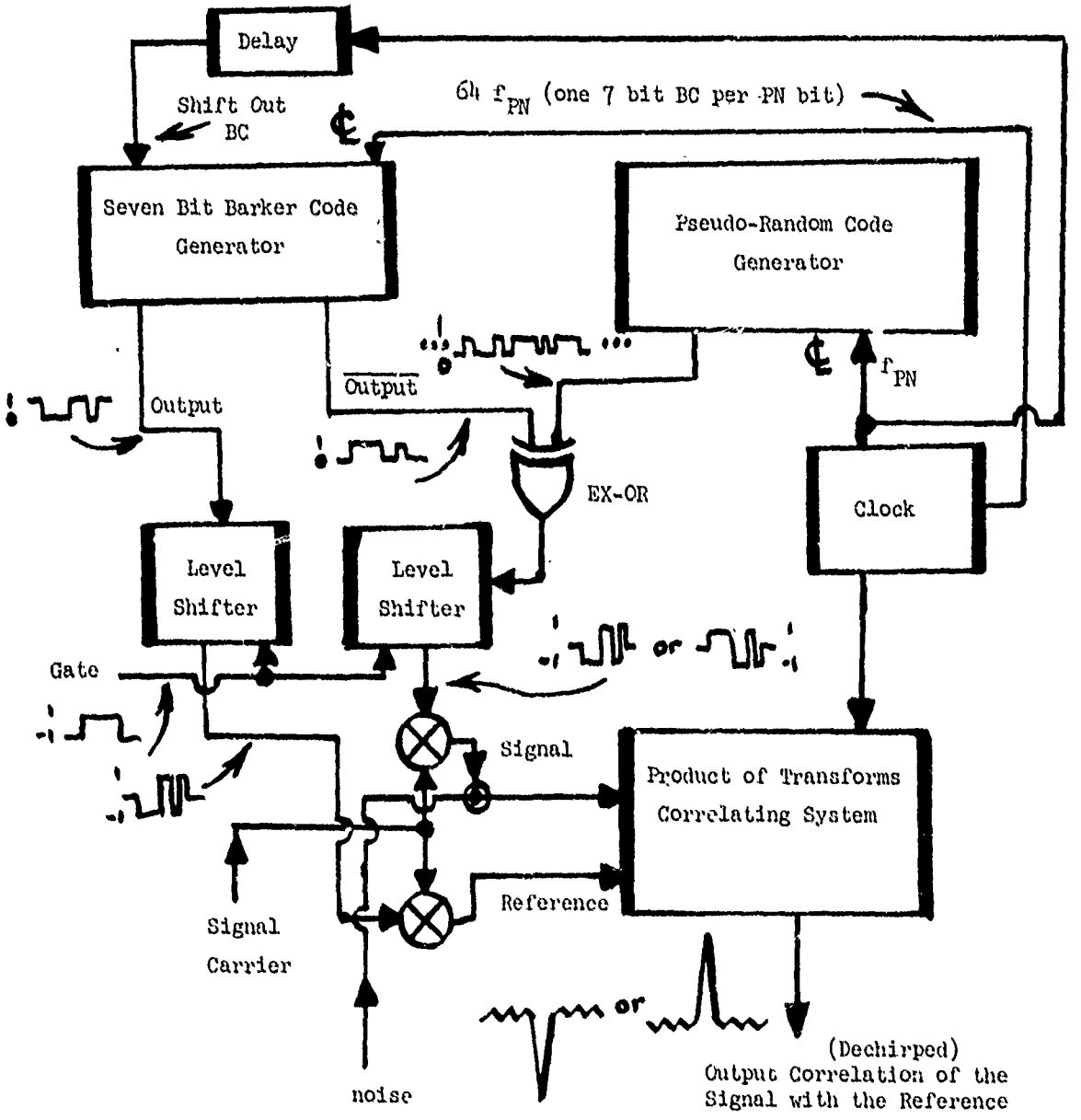

Fig. 14 Block Diagram of the Actual System used in the Error Analysis.

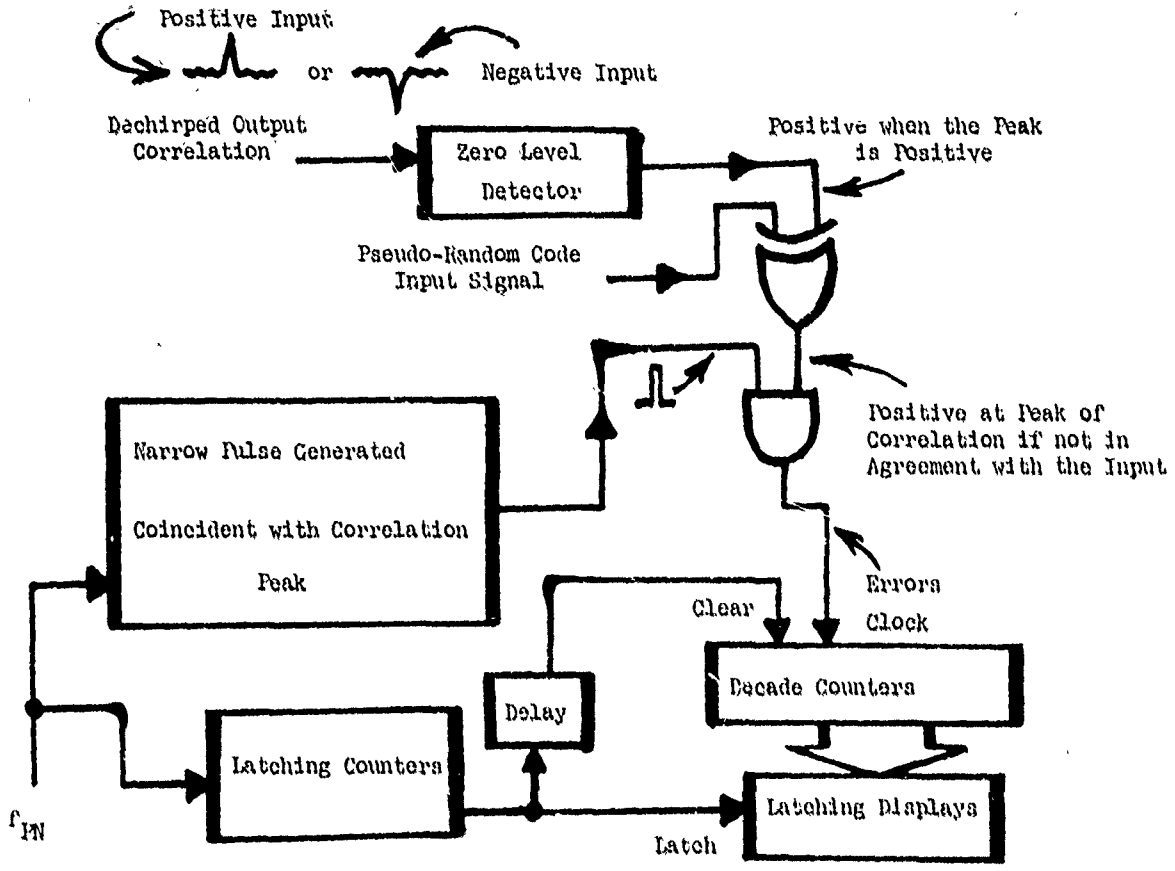

Fig. 15 Block Diagram of the Error Counting Circuitry.

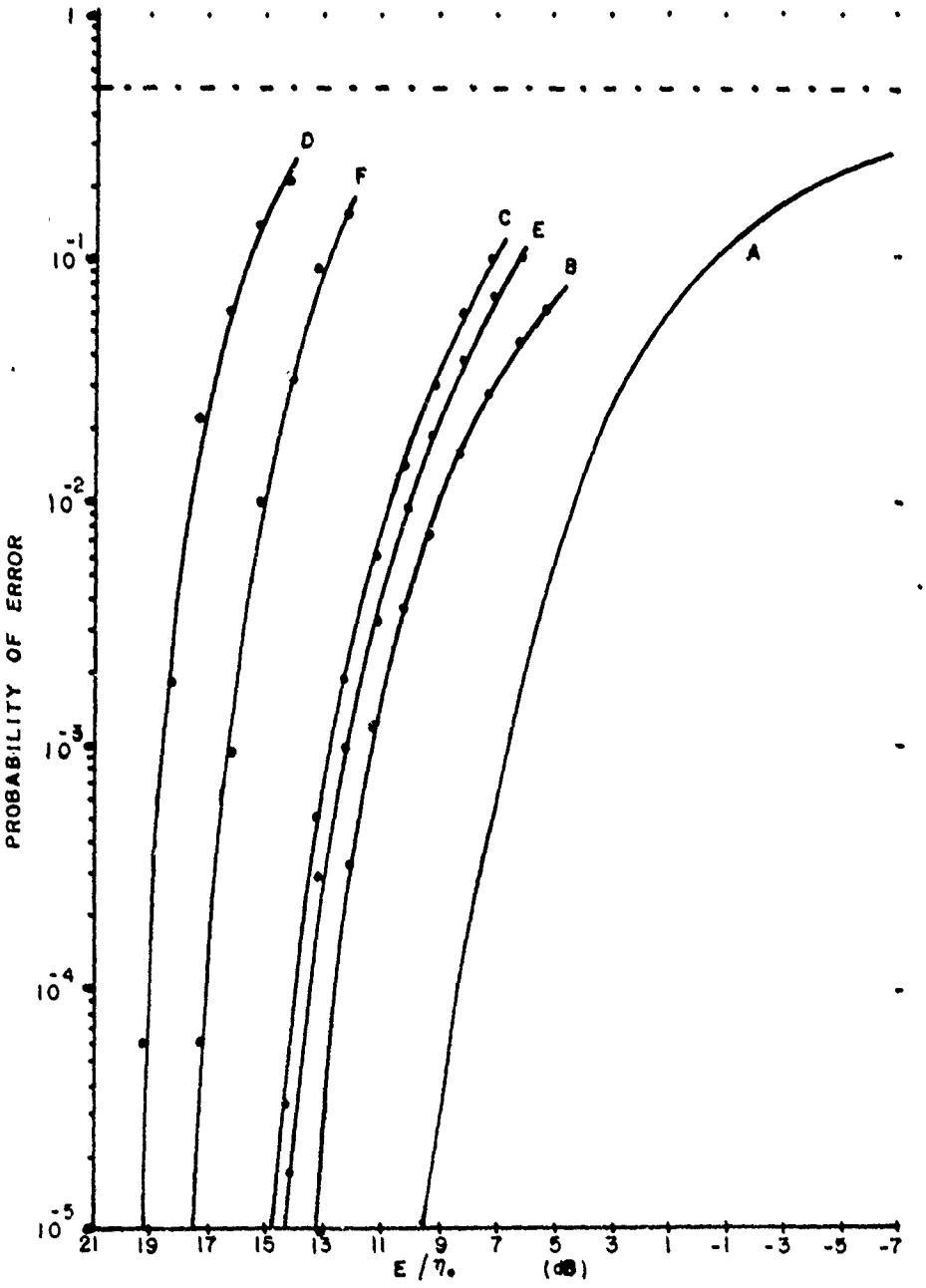

Fig. 16 Probability of Error (PE) Curve for the SAW-Implemented System. Curve A - Optimum Theoretical PE; Curve B - Experimental PE with Approximately White Gaussian Noise; Curve C - Experimental PE for Jammer Level 1.94 dB with Respect to Signal; Curve D - Experimental PE for Jammer Level 9.54 dB with Respect to Signal; Curve E - Same as Curve C, except an Attempt was made to Remove the Jamming; Curve F - Same as Curve D, except an Attempt was made to Remove the Jamming.